

# Dipole Moment Dark Matter at the LHC

Vernon Barger<sup>1</sup>, Wai-Yee Keung<sup>2</sup>, Danny Marfatia<sup>3</sup>, Po-Yan Tseng<sup>1,4</sup>

<sup>1</sup>*Department of Physics, University of Wisconsin, Madison, WI 53706, USA*

<sup>2</sup>*Department of Physics, University of Illinois at Chicago, IL 60607, USA*

<sup>3</sup>*Department of Physics & Astronomy, University of Kansas, Lawrence, KS 66045, USA*

<sup>4</sup>*Department of Physics, National Tsing Hua University, Hsinchu 300, Taiwan*

## Abstract

Monojet and monophoton final states with large missing transverse energy ( $\cancel{E}_T$ ) are important for dark matter (DM) searches at colliders. We present analytic expressions for the differential cross sections for the parton-level processes,  $q\bar{q}(qg) \rightarrow g(q)\chi\bar{\chi}$  and  $q\bar{q} \rightarrow \gamma\chi\bar{\chi}$ , for a neutral DM particle with a magnetic dipole moment (MDM) or an electric dipole moment (EDM). We collectively call such DM candidates dipole moment dark matter (DMDM). We also provide monojet cross sections for scalar, vector and axial-vector interactions. We then use ATLAS/CMS monojet+ $\cancel{E}_T$  data and CMS monophoton+ $\cancel{E}_T$  data to constrain DMDM. We find that 7 TeV LHC bounds on the MDM DM-proton scattering cross section are about six orders of magnitude weaker than on the conventional spin-independent cross section.

## I. INTRODUCTION

Collider data have provided an important avenue for dark matter (DM) searches, especially for candidates lighter than about 10 GeV [1–3], for which direct detection experiments have diminished sensitivity due to the small recoil energy of the scattering process. In fact, current assumption-dependent bounds on spin-dependent DM-nucleon scattering from LHC data, obtained using an effective field theory framework, are comparable or even superior to those from direct detection experiments for DM lighter than a TeV [2, 3].

The final states that have proven to be effective for DM studies at colliders are those with a single jet or single photon and large missing transverse energy ( $\cancel{E}_T$ ) or transverse momentum. Our goal is study these signatures for DM that possesses a magnetic dipole moment (MDM) or an electric dipole moment (EDM) [4]; earlier work can be found in Ref. [5]. Thus, the DM may be a Dirac fermion, but not a Majorana fermion. We refer to these DM candidates as dipole moment dark matter (DMDM). We begin with a derivation of the differential cross sections for the parton-level processes that give monojet+ $\cancel{E}_T$  and monophoton+ $\cancel{E}_T$  final states at the LHC. We then use 7 TeV  $j + \cancel{E}_T$  data from ATLAS [6] and CMS [7], and  $\gamma + \cancel{E}_T$  data from CMS [8] to constrain DMDM. Finally, we place bounds on the MDM DM-proton scattering cross section.

## II. PRODUCTION CROSS SECTIONS

The monojet+ $\cancel{E}_T$  and monophoton+ $\cancel{E}_T$  final states for DM production at the LHC arise from the  $2 \rightarrow 3$  parton level processes  $q\bar{q}(qg) \rightarrow g(q)\chi\bar{\chi}$  and  $q\bar{q} \rightarrow \gamma\chi\bar{\chi}$ . Since the momenta and spin of the final state DM particles can not be measured, their phase space can be integrated out. Thus, the  $2 \rightarrow 3$  processes are simplified to  $2 \rightarrow 2$  processes. We use this fact to find analytic expressions for the parton-level cross sections by first focusing on the DM pair  $\chi\bar{\chi}$ .

A dark matter particle  $\chi$  with magnetic dipole moment  $\mu_\chi$  interacts with an electromagnetic field  $F_{\mu\nu}$  through the interaction  $\mathcal{L} = \frac{1}{2}\mu_\chi\bar{\chi}\sigma^{\mu\nu}F_{\mu\nu}\chi$ . The corresponding vertex is  $\Gamma_M^\mu = \bar{u}(p)i\sigma^{\mu\nu}(p+p')_\nu v(p')$ . Using the Gordon decomposition identity,

$$\bar{u}(p)\gamma^\mu v(p') = \frac{1}{2m_\chi}\bar{u}(p)[p^\mu - p'^\mu + i\sigma^{\mu\nu}(p+p')_\nu]v(p'),$$

we write  $\Gamma_M^\mu$  in terms of the QED scalar annihilation vertex,  $\Gamma_0^\mu = (p-p')^\mu$ , and the QED

vectorial vertex for Dirac fermion pair production,  $\Gamma_{\frac{1}{2}}^\mu = \bar{u}(p)\gamma^\mu v(p')$ :

$$\Gamma_M^\mu = 2m_\chi \Gamma_{\frac{1}{2}}^\mu - \Gamma_0^\mu \bar{u}(p)v(p') .$$

Consider  $\Gamma_0^\mu$ . Integrating the 2-body phase space,

$$dps_2(P = p + p') = (2\pi)^4 \delta^4(P - p - p') \frac{d^3\mathbf{p}}{(2\pi)^3 2E_p} \frac{d^3\mathbf{p}'}{(2\pi)^3 2E_{p'}} ,$$

gives

$$\int dps_2(P = p + p') = \frac{1}{8\pi} \sqrt{1 - 4m_\chi^2/P^2} .$$

The relevant tensor that enters the calculation of the cross section is

$$T_0^{\mu\nu} \equiv \int \Gamma_0^\mu (\Gamma_0^\nu)^* dps_2(P = p + p') .$$

Gauge invariance,  $P_\mu T_0^{\mu\nu} = 0$ , dictates that  $T_0^{\mu\nu}$  take the form,

$$T_0^{\mu\nu} = S_0 (P^2 g^{\mu\nu} - P^\mu P^\nu) .$$

*i.e.*,  $T_0^\mu{}_\mu = 3P^2 S_0$ . Thus to determine  $S_0$ , we can circumvent the more involved tensor calculation by simply evaluating

$$\begin{aligned} T_0^\mu{}_\mu &= \int (p - p')^2 dps_2(P = p + p') = \int (2m_\chi^2 - 2p \cdot p') dps_2 = -\frac{q^2}{8\pi} (1 - 4m_\chi^2/P^2)^{\frac{3}{2}} \\ &\implies S_0 = -\frac{1}{3} \frac{1}{8\pi} (1 - 4m_\chi^2/P^2)^{\frac{3}{2}} . \end{aligned}$$

Now we study  $\Gamma_{\frac{1}{2}}^\mu$ . By analogy to  $T_0^{\mu\nu}$ , we define  $T_{\frac{1}{2}}^{\mu\nu}$  via

$$T_{\frac{1}{2}}^{\mu\nu} \equiv \sum_{spin} \int \Gamma_{\frac{1}{2}}^\mu (\Gamma_{\frac{1}{2}}^\nu)^* dps_2(P = p + p') = S_{\frac{1}{2}} (P^2 g^{\mu\nu} - P^\mu P^\nu) .$$

Taking the trace, we get

$$\begin{aligned} 3P^2 S_{\frac{1}{2}} &= \text{Tr} \int (\not{p} + m_\chi) \gamma^\mu (\not{p}' - m_\chi) \gamma_\mu dps_2 = \text{Tr} \int (-2 \not{p} \not{p}' - 4m_\chi^2 \mathbf{1}) dps_2 \\ &\implies S_{\frac{1}{2}} = -\frac{4}{3} \frac{1}{8\pi} (1 + 2m_\chi^2/P^2) (1 - 4m_\chi^2/P^2)^{\frac{1}{2}} . \end{aligned}$$

In the high energy limit ( $P^2 \gg 4m_\chi^2$ ),  $S_{\frac{1}{2}} = 4S_0$ , as expected by counting degrees of freedom.

The corresponding  $S_M$  for the MDM case can be obtained from the previous calculations and an additional calculation of the interference term,

$$-2(2m_\chi) \text{Tr} (\not{p}' - m_\chi) \gamma^\mu (\not{p} + m_\chi) (p - p')_\mu = -16m_\chi^2 P^2 (1 - 4m_\chi^2/P^2) .$$

We find

$$S_M = 4m_\chi^2 S_{\frac{1}{2}} + 2q^2(1 - 4m_\chi^2/q^2)S_0 + S_X,$$

with  $S_X = -\frac{16}{3}\frac{1}{8\pi}m_\chi^2(1 - 4m_\chi^2/q^2)^{\frac{3}{2}}$ . Therefore,

$$S_M = -\frac{2}{3}\frac{1}{8\pi}P^2(1 + 8m_\chi^2/P^2)\sqrt{1 - 4m_\chi^2/P^2}.$$

We are interested in e.g.,  $q(p_1) + \bar{q}(p_2) \rightarrow g(p_3) + [\chi\bar{\chi}](P)$ , with  $s = (p_1 + p_2)^2$ ,  $t = (p_1 - p_3)^2$ ,  $u = (p_2 - p_3)^2$ , and  $s + t + u = P^2$ , the invariant mass squared of the DM pair  $\chi\bar{\chi}$ . This defines our notation. Multiplying the cross sections for Drell-Yan at high  $p_T$  [9] by  $S_M(m_\chi)/S_{\frac{1}{2}}(m_\ell = 0)$  (with an appropriate modification of couplings), we obtain

$$\frac{d\sigma^{MDM}}{dt dP^2}(q\bar{q} \rightarrow b[\chi\bar{\chi}]) = \frac{C_b e^2 e_q^2}{16\pi s^2} \frac{\mu_\chi^2}{24\pi^2} \frac{8(t - P^2)^2 + (u - P^2)^2}{9 tu} \left(1 + \frac{8m_\chi^2}{P^2}\right) \left(1 - \frac{4m_\chi^2}{P^2}\right)^{\frac{1}{2}}, \quad (1)$$

$$\frac{d\sigma^{MDM}}{dt dP^2}(qg \rightarrow q[\chi\bar{\chi}]) = \frac{g_s^2 e^2 e_q^2}{16\pi s^2} \frac{\mu_\chi^2}{24\pi^2} \frac{1}{3} \frac{(u - P^2)^2 + (s - P^2)^2}{-su} \left(1 + \frac{8m_\chi^2}{P^2}\right) \left(1 - \frac{4m_\chi^2}{P^2}\right)^{\frac{1}{2}}, \quad (2)$$

where  $e_q$  is the quark charge in units of  $e$ . If the gauge boson  $b$  is a gluon,  $C_b = g_s^2$ , and if it is a photon,  $C_b = \frac{3}{4}e_q^2 e^2$ .

The interaction Lagrangian for a DM particle with EDM  $d_\chi$  is  $\mathcal{L} = \frac{1}{2}d_\chi \bar{\chi} \sigma^{\mu\nu} \gamma_5 F_{\mu\nu} \chi$ . A similar procedure gives the EDM DM cross sections,

$$\frac{d\sigma^{EDM}}{dt dP^2}(q\bar{q} \rightarrow b[\chi\bar{\chi}]) = \frac{C_b e^2 e_q^2}{16\pi s^2} \frac{d_\chi^2}{24\pi^2} \frac{8(t - P^2)^2 + (u - P^2)^2}{9 tu} \left(1 - \frac{4m_\chi^2}{P^2}\right)^{\frac{3}{2}}, \quad (3)$$

$$\frac{d\sigma^{EDM}}{dt dP^2}(qg \rightarrow q[\chi\bar{\chi}]) = \frac{g_s^2 e^2 e_q^2}{16\pi s^2} \frac{d_\chi^2}{24\pi^2} \frac{1}{3} \frac{(u - P^2)^2 + (s - P^2)^2}{-su} \left(1 - \frac{4m_\chi^2}{P^2}\right)^{\frac{3}{2}}. \quad (4)$$

DMDM interacts with the  $Z$ -boson via the relevant dimension-5 Lagrangian,  $\mathcal{L} = \frac{1}{2}\bar{\chi}\sigma^{\mu\nu}(d_B + d_E\gamma_5)\chi Z_{\mu\nu}$ , where  $Z_{\mu\nu} = \partial_\mu Z_\nu - \partial_\nu Z_\mu$ . The fermion line of the final DM state is

$$\Gamma_Z^\mu = \bar{u}(p)\sigma^{\mu\rho}(d_B + d_E\gamma_5)(p + p')_\rho v(p').$$

On doing the phase space integration, the following tensor appears:

$$T_Z^{\mu\nu} = \sum_{spin} \int \Gamma_Z^\mu (\Gamma_Z^\nu)^\dagger dp s_2 = S_Z (P^2 g^{\mu\nu} + P^\mu P^\nu).$$

Its trace is

$$T_Z^\mu{}_\mu = 3P^2 S_Z = (-\pi P^4) \frac{1}{(2\pi)^2} \left[ d_B^2 \left(1 + \frac{8m_\chi^2}{P^2}\right) + d_E^2 \left(1 - \frac{4m_\chi^2}{P^2}\right) \right] \left(1 - \frac{4m_\chi^2}{P^2}\right)^{\frac{1}{2}},$$

$$\implies S_Z = -\frac{\pi}{3} P^2 \frac{1}{(2\pi)^2} \left[ d_B^2 \left( 1 + \frac{8m_\chi^2}{P^2} \right) + d_E^2 \left( 1 - \frac{4m_\chi^2}{P^2} \right) \right] \left( 1 - \frac{4m_\chi^2}{P^2} \right)^{\frac{1}{2}}.$$

In general, we expect interference from the photon MDM  $\mu_\chi$  and EDM  $d_\chi$  amplitudes. After integrating out the two-body phase space of the final state DM, the differential cross sections are

$$\begin{aligned} \frac{d\sigma^{\gamma,Z}}{dt dP^2}(q\bar{q} \rightarrow g[\bar{\chi}\chi]) &= \frac{1}{16\pi s^2} \frac{g_s^2 e^2}{27\pi^2} \frac{(P^2 - u)^2 + (P^2 - t)^2}{tu} \left( 1 - \frac{4m_\chi^2}{P^2} \right)^{\frac{1}{2}} \\ &\times \sum_{i=E,B} \left( 1 + \frac{F_i m_\chi^2}{P^2} \right) P^4 \left[ \left| \frac{g_A^q d_i}{P^2 - M_Z^2 + iM_Z \Gamma_Z} \right|^2 \right. \\ &\quad \left. + \left| \frac{e_q d_i^\gamma}{P^2} + \frac{g_V^q d_i}{P^2 - M_Z^2 + iM_Z \Gamma_Z} \right|^2 \right], \end{aligned} \quad (5)$$

$$\begin{aligned} \frac{d\sigma^{\gamma,Z}}{dt dP^2}(qg \rightarrow q[\bar{\chi}\chi]) &= \frac{1}{16\pi s^2} \frac{g_s^2 e^2}{72\pi^2} \frac{(P^2 - u)^2 + (P^2 - s)^2}{-su} \left( 1 - \frac{4m_\chi^2}{P^2} \right)^{\frac{1}{2}} \\ &\times \sum_{i=E,B} \left( 1 + \frac{F_i m_\chi^2}{P^2} \right) P^4 \left[ \left| \frac{g_A^q d_i}{P^2 - M_Z^2 + iM_Z \Gamma_Z} \right|^2 \right. \\ &\quad \left. + \left| \frac{e_q d_i^\gamma}{P^2} + \frac{g_V^q d_i}{P^2 - M_Z^2 + iM_Z \Gamma_Z} \right|^2 \right], \end{aligned} \quad (6)$$

where we use the notation,  $d_B^\gamma \equiv \mu_\chi$  and  $d_E^\gamma \equiv d_\chi$ , to keep Eqs. (5) and (6) compact. Here,  $F_B = 8$ ,  $F_E = -4$ , and  $x_W = \sin^2 \vartheta_W \approx 0.23$ ,  $g_V^q \sin \vartheta_W \cos \vartheta_W = \frac{1}{2}(T_3^q)_L - e_q \sin^2 \vartheta_W$  and  $g_A^q \sin \vartheta_W \cos \vartheta_W = -\frac{1}{2}(T_3^q)_L$  define the quark- $Z$  boson couplings. In what follows, we set  $d_B = d_E = 0$ .

For the sake of completeness, we also work out the monojet cross sections for the scalar, vector, and axial-vector interactions. The amplitudes are  $G_{q,0}(\bar{q}q)(\bar{\chi}\chi)$ ,  $G_{q,V}(\bar{q}\gamma_\mu q)(\bar{\chi}\gamma^\mu \chi)$ , and  $G_{q,A}(\bar{q}\gamma_\mu \gamma_5 q)(\bar{\chi}\gamma^\mu \gamma_5 \chi)$ , respectively.

For the scalar case,

$$\frac{d\sigma^S}{dt dP^2}(q\bar{q} \rightarrow g[\chi\bar{\chi}]) = \frac{g_s^2 G_{q,0}^2}{16\pi s^2} \frac{P^2}{16\pi^2} \frac{8s^2 + P^2}{9tu} \left( 1 - \frac{4m_\chi^2}{P^2} \right)^{\frac{3}{2}}, \quad (7)$$

$$\frac{d\sigma^S}{dt dP^2}(qg \rightarrow q[\chi\bar{\chi}]) = \frac{g_s^2 G_{q,0}^2}{16\pi s^2} \frac{P^2}{16\pi^2} \frac{1}{3} \frac{t^2 + P^2}{-su} \left( 1 - \frac{4m_\chi^2}{P^2} \right)^{\frac{3}{2}}. \quad (8)$$

For the vector case,

$$\frac{d\sigma^V}{dt dP^2}(q\bar{q} \rightarrow g[\chi\bar{\chi}]) = \frac{g_s^2 G_{q,V}^2}{16\pi s^2} \frac{P^2}{12\pi^2} \frac{8}{9} \frac{(t - P^2)^2 + (u - P^2)^2}{tu} \left( 1 - \frac{4m_\chi^2}{P^2} \right)^{\frac{1}{2}} \left( 1 + \frac{2m_\chi^2}{P^2} \right), \quad (9)$$

$$\frac{d\sigma^V}{dt dP^2}(qg \rightarrow q[\chi\bar{\chi}]) = \frac{g_s^2 G_{q,V}^2}{16\pi s^2} \frac{P^2}{12\pi^2} \frac{1}{3} \frac{(s-P^2)^2 + (u-P^2)^2}{-su} \left(1 - \frac{4m_\chi^2}{P^2}\right)^{\frac{1}{2}} \left(1 + \frac{2m_\chi^2}{P^2}\right). \quad (10)$$

For the axial-vector case,

$$\frac{d\sigma^{AV}}{dt dP^2}(q\bar{q} \rightarrow g[\chi\bar{\chi}]) = \frac{g_s^2 G_{q,A}^2}{16\pi s^2} \frac{P^2}{12\pi^2} \frac{8}{9} \frac{(t-P^2)^2 + (u-P^2)^2}{tu} \left(1 - \frac{4m_\chi^2}{P^2}\right)^{\frac{3}{2}}, \quad (11)$$

$$\frac{d\sigma^{AV}}{dt dP^2}(qg \rightarrow q[\chi\bar{\chi}]) = \frac{g_s^2 G_{q,A}^2}{16\pi s^2} \frac{P^2}{12\pi^2} \frac{1}{3} \frac{(s-P^2)^2 + (u-P^2)^2}{-su} \left(1 - \frac{4m_\chi^2}{P^2}\right)^{\frac{3}{2}}. \quad (12)$$

The kinematic limits for the subprocess are  $P^2 \in [(2m_\chi)^2, s]$ ,  $-t \in [0, s - P^2]$ . For  $\cancel{p}_T$  cuts, there are additional kinematic constraints.

The above equations apply for Dirac fermion DM. For Majorana DM, there are only scalar and axial-vector interactions. All the other interactions are absent. The results for Majorana DM can be obtained from the corresponding equations by dividing by 2 (since the 2-body phase space for two identical particles is half that for two distinct particles).

### III. CONSTRAINTS

The vertices defining DMDM interactions with the electromagnetic field are

$$V_{\gamma\chi\bar{\chi}}(MDM) = \frac{e}{\Lambda_{MDM}} \sigma^{\mu\alpha} P_\mu,$$

$$V_{\gamma\chi\bar{\chi}}(EDM) = \frac{e}{\Lambda_{EDM}} \sigma^{\mu\alpha} P_\mu \gamma_5,$$

where  $P$  is the photon's 4-momentum vector and  $\alpha$  is the Dirac index of the photon field. The effective cutoff scales  $\Lambda_{MDM}$  and  $\Lambda_{EDM}$  are defined so that  $\mu_\chi = e/\Lambda_{MDM}$  and  $d_\chi = e/\Lambda_{EDM}$ , in order to facilitate comparison. They may be related to compositeness or short distance physics, but are not necessarily new physics scales.

Since monojet +  $\cancel{E}_T$  data from ATLAS and CMS [6, 7], and monophoton +  $\cancel{E}_T$  data from CMS [8], at the 7 TeV LHC, are consistent with the SM, we may use these data to constrain the DMDM cutoff scales. From an analysis of 1/fb of monojet data, with the requirement that the hardest jet have  $p_T > 350$  GeV, or  $p_T > 250$  GeV, or  $p_T > 120$  GeV, and pseudorapidity  $|\eta| < 2$ , the ATLAS collaboration has placed 95% C.L. upper limits on the production cross section of 0.035 pb, 0.11 pb and 1.7 pb, respectively [6]. In 5/fb of data, CMS has observed 1142 monojet events with leading jet  $p_T > 350$  GeV and  $|\eta| < 2.4$  [7], to be compared

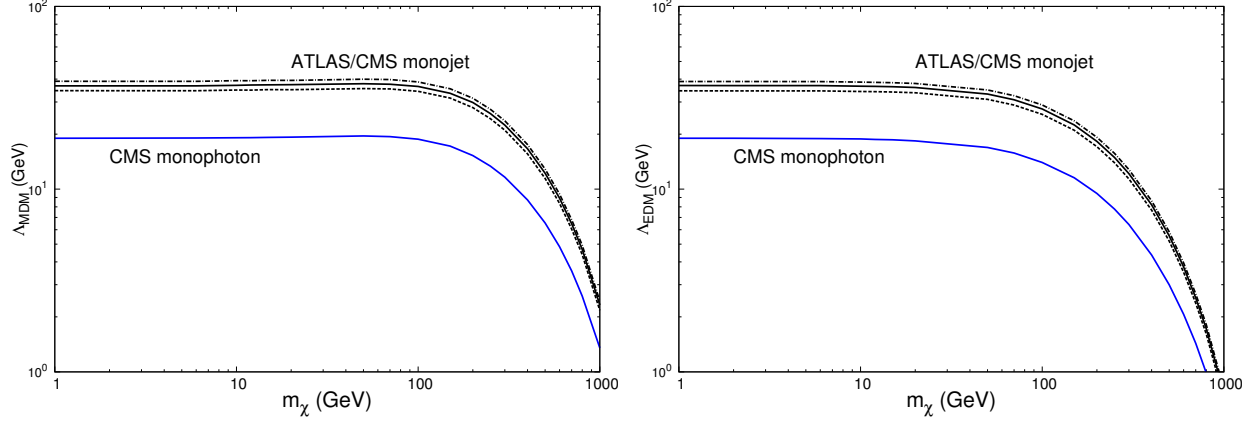


FIG. 1. The black lines are the 95% C.L. lower limits on the cutoff scales from ATLAS (solid) and CMS (dash-dotted: observed, dashed: expected) monojet data with leading jet  $p_T > 350$  GeV and  $|\eta| < 2$  for ATLAS and  $|\eta| < 2.4$  for CMS, and the solid blue lines are the 90% C.L. lower limits from the CMS monophoton data.

with the standard model (SM) expectation,  $N_{SM} \pm \sigma_{SM} = 1225 \pm 101$ . We will calculate both observed and expected 95% C.L. upper limits from CMS monojet data. Using 5/fb data, CMS has searched for the  $\gamma + \cancel{E}_T$  final state with photon  $p_T > 145$  GeV and  $|\eta| < 1.44$ , and set a 90% C.L. upper limit on the production cross section of about 0.0143 pb [8].

To place constraints using the total event rate, we calculate the cross sections relevant to each detector,  $\sigma_{ATLAS}$  and  $\sigma_{CMS}$ , of the processes  $q\bar{q} \rightarrow g\chi\bar{\chi}$ ,  $qg \rightarrow q\chi\bar{\chi}$  and  $q\bar{q} \rightarrow \gamma\chi\bar{\chi}$ , by convolving Eqs. (1)-(4) with the parton distribution functions from CTEQ6 [10]. For MDM DM, we have checked that we get the same results from a calculation that begins with an evaluation of the amplitude squared and the 3-body phase space. Using CMS  $j + \cancel{E}_T$  data, we place 95% C.L. lower limits on the cutoff scales by requiring [3]

$$\chi^2 \equiv \frac{[\Delta_N - N_{DM}(m_\chi, \Lambda)]^2}{N_{DM}(m_\chi, \Lambda) + N_{SM} + \sigma_{SM}^2} = 3.84,$$

where [7]

$$\Delta_N = \begin{cases} 200 & \text{expected bound} \\ 158 & \text{observed bound} \end{cases},$$

and  $N_{DM}(m_\chi, \Lambda) = \sigma_{CMS} \times \text{luminosity}$ . The above-mentioned bounds on the production cross sections obtained by the ATLAS and CMS collaborations from the  $j + \cancel{E}_T$  and  $\gamma + \cancel{E}_T$  final states can be used directly to constrain the cutoff scales. Figure 1 shows lower limits on  $\Lambda_{MDM}$  and  $\Lambda_{EDM}$ ; the bound from ATLAS corresponds to the  $p_T > 350$  GeV cut on the

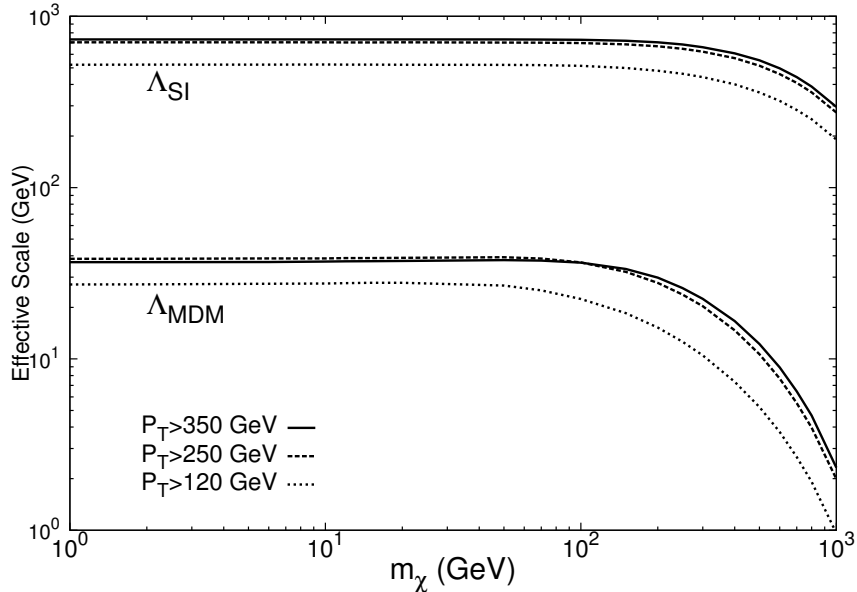


FIG. 2. 95% C.L. lower limits from ATLAS  $j + \cancel{E}_T$  data on  $\Lambda_{SI}$  and  $\Lambda_{MDM}$ .

hardest jet. We see that for  $m_\chi < 100$  GeV, the 95% C.L. lower limit on the cutoff scales is only about 35 GeV. For conventional spin-independent (SI) amplitudes of dimension-6, e.g.,

$$(\bar{q}\gamma_\mu q)(\bar{\chi}\gamma^\mu\chi)/\Lambda_{SI}^2, \quad q = u, d \quad (13)$$

typical bounds on  $\Lambda_{SI}$  are a few hundred GeV for  $m_\chi < 100$  GeV, as shown in Fig. 2. The result is counterintuitive since we naively expect the lower limit on  $\Lambda_{MDM}$  and  $\Lambda_{EDM}$  to be stronger than on  $\Lambda_{SI}$  since the DMDM operators are dimension-5. We now explain this result.

Consider MDM DM and the amplitude of Eq. (13). Neglecting  $m_\chi$ , and evaluating the cross sections at the peak of the product of the phase space and PDFs for a chosen  $p_T$  cut, we find

$$\frac{\sigma^{SI}(pp \rightarrow j + \cancel{E}_T)}{\sigma^{MDM}(pp \rightarrow j + \cancel{E}_T)} \approx \frac{8p_T^2\Lambda_{MDM}^2}{e^4\Lambda_{SI}^4}.$$

The left hand side of the equation is unity for an experimental upper bound on the cross section. Then, the lower bound on  $\Lambda_{MDM}$  for a known lower bound on  $\Lambda_{SI}$  is  $e^2\Lambda_{SI}^2/(2\sqrt{2}p_T)$ . From Fig. 2, the 95% C.L. lower limit on  $\Lambda_{SI}$  is 700 GeV for a  $p_T$  cut of 350 GeV, which translates into a 95% C.L. lower limit on  $\Lambda_{MDM}$  of 45 GeV.



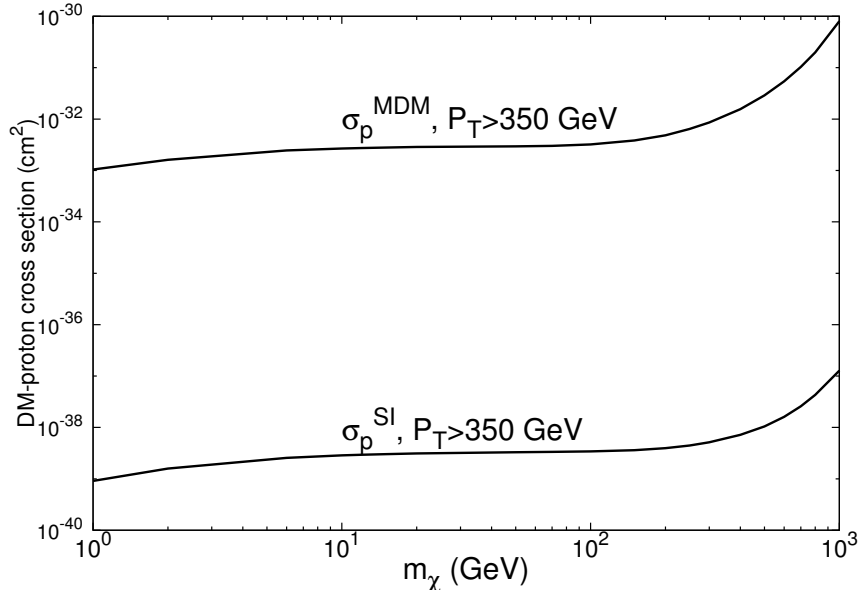


FIG. 3. 95% C.L. upper limits on the conventional SI and MDM DM-proton cross sections from ATLAS  $j + \cancel{E}_T$  data.

#### IV. SCATTERING CROSS SECTIONS

Including the SI and spin-dependent contributions, and setting the electric and magnetic form factors to unity, the MDM DM-proton cross section is [11, 12]<sup>1</sup>

$$\sigma_p^{MDM} = \frac{e^4}{2\pi\Lambda_{MDM}^2} \left( 1 - \frac{m_r^2}{2m_p^2} - \frac{m_r^2}{m_p m_\chi} + \left( \frac{\mu_p}{\frac{e}{2m_p}} \right)^2 \frac{m_r^2}{m_p^2} \right),$$

where  $m_r = \frac{m_\chi m_p}{m_\chi + m_p}$  is the reduced mass of the DM-proton system, and  $\mu_p = 2.793e/(2m_p)$  is the MDM of the proton [13]. We employ the 95% C.L. lower limit on  $\Lambda_{MDM}$  obtained in Fig. 1 from ATLAS data, to determine the 95% C.L. upper limit on the MDM DM-proton cross section  $\sigma_p^{MDM}$ . This is shown in Fig. 3.

We now relate limits from the  $j + \cancel{E}_T$  final state on the MDM DM-proton scattering cross section to limits on the conventional SI DM-proton cross section. The DM-proton scattering cross section for the amplitude of Eq. (13) is

$$\sigma_p^{SI} = \frac{9m_r^2}{\pi\Lambda_{SI}^4}.$$

<sup>1</sup> The total cross section is divergent since the Coulomb interaction is singular. Here, we use the energy transfer cross section [12] that is the same as the usual total cross section for constant differential cross sections.

The 95% C.L. upper limit on  $\sigma_p^{SI}$  from ATLAS data is shown in Fig. 3. Note that the constraint on  $\sigma_p^{SI}$  is about six orders of magnitude more stringent than on  $\sigma_p^{MDM}$ . This is evident from

$$\frac{\sigma_p^{SI}}{\sigma_p^{MDM}} \approx \frac{2m_p^2 \Lambda_{MDM}^2}{e^4 \Lambda_{SI}^4},$$

with the limits on  $\Lambda_{MDM}$  and  $\Lambda_{SI}$  from Fig. 2.

The CoGeNT event excess [14] can be explained by a 7 GeV DM particle with a MDM with  $\Lambda_{MDM} = 3$  TeV [11]. In fact, this candidate can also explain the signals seen by the DAMA [15] and CRESST [16] experiments, and may survive conservative bounds from other direct detection experiments [17]. From Fig. 1, we conclude that LHC bounds are far from ruling out this candidate. This is in contrast to conventional SI scattering, which for light DM, finds strong constraints in collider experiments.

## ACKNOWLEDGMENTS

This work was supported by the DoE under Grant Nos. DE-FG02-12ER41811, DE-FG02-95ER40896 and DE-FG02-04ER41308, by the NSF under Grant No. PHY-0544278, by the National Science Council of Taiwan under Grant No. 100-2917-I-007-002, and by the WARF.

- 
- [1] J. Goodman, M. Ibe, A. Rajaraman, W. Shepherd, T. M. P. Tait and H.-B. Yu, Phys. Lett. B **695**, 185 (2011) [arXiv:1005.1286 [hep-ph]]; Y. Bai, P. J. Fox and R. Harnik, JHEP **1012**, 048 (2010) [arXiv:1005.3797 [hep-ph]]; J. Goodman, M. Ibe, A. Rajaraman, W. Shepherd, T. M. P. Tait and H.-B. Yu, Phys. Rev. D **82**, 116010 (2010) [arXiv:1008.1783 [hep-ph]]; P. J. Fox, R. Harnik, J. Kopp and Y. Tsai, Phys. Rev. D **84**, 014028 (2011) [arXiv:1103.0240 [hep-ph]]; K. Cheung, P.-Y. Tseng, Y.-L. S. Tsai and T.-C. Yuan, JCAP **1205**, 001 (2012) [arXiv:1201.3402 [hep-ph]].
- [2] A. Rajaraman, W. Shepherd, T. M. P. Tait and A. M. Wijangco, Phys. Rev. D **84**, 095013 (2011) [arXiv:1108.1196 [hep-ph]].
- [3] P. J. Fox, R. Harnik, J. Kopp and Y. Tsai, Phys. Rev. D **85**, 056011 (2012) [arXiv:1109.4398 [hep-ph]]; P. J. Fox, R. Harnik, R. Primulando and C.-T. Yu, arXiv:1203.1662 [hep-ph].

- [4] K. Sigurdson, M. Doran, A. Kurylov, R. R. Caldwell and M. Kamionkowski, Phys. Rev. D **70**, 083501 (2004) [Erratum-ibid. D **73**, 089903 (2006)] [arXiv:astro-ph/0406355]. Variations on the theme exist, *e.g.*, B. Feldstein, P. W. Graham and S. Rajendran, Phys. Rev. D **82**, 075019 (2010) [arXiv:1008.1988 [hep-ph]].
- [5] J.-F. Fortin and T. M. P. Tait, Phys. Rev. D **85**, 063506 (2012) [arXiv:1103.3289 [hep-ph]].
- [6] M. Martinez *et al.* [ATLAS Collaboration], arXiv:1202.0158 [hep-ex].
- [7] S. Chatrchyan *et al.* [CMS Collaboration], arXiv:1206.5663 [hep-ex].
- [8] S. Chatrchyan *et al.* [CMS Collaboration], arXiv:1204.0821 [hep-ex].
- [9] See *e.g.*, R. D. Field, *Applications of Perturbative QCD*, Addison-Wesley Publishing Company, The Advanced Book Program, 1989.
- [10] J. Pumplin, A. Belyaev, J. Huston, D. Stump and W. K. Tung, JHEP **0602**, 032 (2006) [hep-ph/0512167].
- [11] V. Barger, W.-Y. Keung and D. Marfatia, Phys. Lett. B **696**, 74 (2011) [arXiv:1007.4345 [hep-ph]].
- [12] S. A. Raby and G. West, Nucl. Phys. B **292**, 793 (1987).
- [13] <http://www.webelements.com/hydrogen/isotopes.html>
- [14] C. E. Aalseth *et al.* [CoGeNT Collaboration], Phys. Rev. Lett. **106**, 131301 (2011) [arXiv:1002.4703 [astro-ph.CO]].
- [15] R. Bernabei *et al.* [DAMA Collaboration], Eur. Phys. J. C **56**, 333 (2008) [arXiv:0804.2741 [astro-ph]].
- [16] G. Angloher, M. Bauer, I. Bavykina, A. Bento, C. Bucci, C. Ciemniak, G. Deuter and F. von Feilitzsch *et al.*, Eur. Phys. J. C **72**, 1971 (2012) [arXiv:1109.0702 [astro-ph.CO]].
- [17] E. Del Nobile, C. Kouvaris, P. Panci, F. Sannino and J. Virkajarvi, arXiv:1203.6652 [hep-ph].